

Surface critical behaviors of coupled Haldane chains

Wenjing Zhu,¹ Chengxiang Ding,² Long Zhang,³ and Wenan Guo^{1,4,*}

¹*Department of Physics, Beijing Normal University, Beijing 100875, China*

²*School of Science and Engineering of Mathematics and Physics,
Anhui University of Technology, Maanshan, Anhui 243002, China*

³*Kavli Institute for Theoretical Sciences and CAS Center for Excellence in Topological Quantum Computation,
University of Chinese Academy of Sciences, Beijing 100190, China*

⁴*Beijing Computational Science Research Center, Beijing 100193, China*

(Dated: October 22, 2020)

The special surface transition at (2+1)-dimensional quantum critical point is precluded in corresponding classical critical point. The mechanism of such behavior which is only found in dimerized Heisenberg models so far is still under debate. To illuminate the role of symmetry protected topological (SPT) phase in inducing such nonordinary behaviors, we study a system on a two-dimensional square lattice consisted by interacting spin-1 Haldane chains, which has a genuine SPT phase—the Haldane phase—at weak interchain interactions and a quantum critical point belonging to the classical 3D O(3) universality class to the Néel phase. Different from models studied previously, there is no dimerization in the current model. Cutting the system along the chain direction or perpendicular to the chain direction exposes two different surfaces. Using unbiased quantum Monte Carlo simulations, we find that the two different types of surface show completely different surface critical behaviors at the bulk critical point, resulted from different surface states in the SPT phase. For the system with surfaces along the chain direction, the surface critical behavior is of ordinary type of the bulk 3D O(3) critical point, while for the surfaces perpendicular to the chain direction, the surface critical behavior is nonordinary, consistent with special transitions found in dimerized Heisenberg models. Our numerical results demonstrate that the gapless surface state in the gapped SPT phase together with the gapless mode of critical point is a pure quantum scenario that leads to the nonordinary transition.

PACS numbers: to be added

I. INTRODUCTION

The field of classical surface criticality behavior (SCB) is rather mature. [1, 2] It is well known and understood well based on the renormalization group theory [3] that, by tuning the surface coupling, different surface universality classes can be realized. In particular, in the case that the surface can hold a long-range order, e.g., the two-dimensional (2D) surface of the three-dimensional (3D) Ising model, three different SCB universality classes: ordinary, extraordinary and special transitions, can be realized. But for models with continuous symmetry that can not hold a long-range order on the surface at finite temperature due to Mermin-Wagner theorem, [4] e.g. the 2D surface of a 3D O(n) model with $n \geq 3$, it is widely accepted that there is neither extraordinary nor special transition. According to the quantum to classical mapping valid in particular to unfrustrated quantum antiferromagnets(AF), the d -dimensional SU(2) quantum critical point can be described by a $(d+1)$ -dimensional classical effective O(3) Ginzburg-Landau theory. [5] We thus expect that there is neither special nor extraordinary surface transition at the 2D SU(2) quantum critical points.

However, a nonordinary SCB was found in the 2D Affleck-Kennedy-Lieb-Tasaki (AKLT)[6] to Néel quan-

tum critical point, which belongs to the 3D O(3) universality class, recently. [7] The bulk quantum criticality is realized by the spin-1/2 AF Heisenberg (AFH) model on a decorated square lattice (DS). The surface transition has exponents different from those of the ordinary transition of the 3D O(3) critical point, suggesting that an impossible SCB happens at the quantum critical point, denying the quantum to classical correspondence. Such an unusual behavior was attributed to the symmetry-protected topological (SPT) [8, 9] phase which, in contrast to the trivial (non-SPT) disordered phase, has gapless surface states. At quantum critical point, such pure quantum originated gapless states together with the gapless critical modes leads to unconventional SCB.[7]

This discovery has inspired further interests in the investigation on SCBs with pure quantum origin. Ding et al [10] found that different ways of cutting 2D periodic dimerized Heisenberg models on the square lattice into systems with boundaries can lead to all three types of SCB universality at the bulk quantum critical points which belong to the 3D O(3) universality class. In particular, for the columnar dimerized Heisenberg model, system with surfaces formed by non-dangling spins shows SCB corresponding to the ordinary transition of the 3D O(3) class, while, remarkably, system with surfaces formed by dangling spins shows nonordinary SCB, with exponents in agreement with the special transition of the 3D O(3) class— numerical values of the exponents are close to those obtained by the renormalization-group cal-

* waguo@bnu.edu.cn

culations for the special surface transition of the 3D O(3) model. Similar results are obtained by Weber et al [11] independently.

Furthermore, Weber and collaborators studied the SCB at the same quantum critical point between the AKLT phase and the Néel phase of the spin-1/2 Heisenberg model on the DS lattice studied in 7 but with different cut introduced. They found that the system shows the ordinary SCB on the non-dangling surface, although it shows the same nonordinary transition as that found by Zhang and Wang [7] on the dangling surface. This finding challenges the role of SPT in the origin of nonordinary SCBs. In addition, they studied another quantum critical point separating the plaquette valence-bond crystal (PVBC) phase and the Néel phase of the same model. Nonordinary and ordinary transitions are again found at the dangling and nondangling surfaces, respectively.

The exponents for the nonordinary transitions among various models agree well, therefore they are taken as an indication for a distinct universality class: the special transition of the 3D O(3) class. Nevertheless it was also observed that the exponents varies upon perturbations, thus the universality is less universal than previously anticipated.[12]

Although it is apparent that the nonordinary SCBs have purely quantum origin, the mechanism is not clear yet. One possible scenario is that the dangling surface forms spin-1/2 AFH chain. Because of the topological θ -term, the proliferation of topological defects in the corresponding classical field theory are suppressed and the surface captures the gapless state, complemented with the critical mode of the bulk, this leads to the special transition[10, 11]. However, a recent work by Weber and Wessel[12] shows that this scenario is problematic: the dangling surface of spin-1 AF Heisenberg model also shows unexpected nonordinary surface transition. The role of SPT in the nonordinary SCB, which was challenged [10, 11], as mentioned in previous text, was further objected by the finding that the suggested AKLT phase of the spin-1/2 Heisenberg model on the DS lattice can be adiabatically connected to the quantum-disorder state of the bilayer Heisenberg model on square lattice without breaking any symmetries, which suggests that the disordered phase is not a real SPT phase. [11]

In consideration of the current confusing situation, it is good to study a model with a genuine SPT phase separated from the Néel phase by a quantum critical point that belongs to the 3D O(3) universality class and to investigate if there is a nonordinary SCB related to the SPT gapless surface mode, but has nothing to do with dimerization, which defines the dangling and non-dangling edges of spins. In this work, we study coupled Haldane chains forming a 2D square lattice, with intrachain interaction J_y and interchain interaction J_x , as shown in Fig. 1. The model describes materials that attracted considerable research [13–25].

In one dimension (1D), the Haldane phase [26, 27] with the SPT order [8, 9] is characterized by nonlocal string

order [28] parameter. With open boundaries, the Haldane chain carries gapless spin-1/2 excitation. This is easy to understand from the AKLT state by deforming $S = 1$ spin into two $S = 1/2$ spins. In 2D, the model has a gapped Haldane phase for $J_x \ll J_y$. Although the string order parameter is argued to decay exponentially for arbitrarily small interchain coupling[29], it is demonstrated that the Haldane phase remains a nontrivial SPT state for small but finite interchain coupling. [30] It is clear that the model can be adiabatically connected to the Haldane phase in 1D as $J_x \rightarrow 0$. As a result, the system should be able to present nontrivial surface states that are either gapless or degenerate edge states. The spatial inversion symmetry about the chain protects edge states of surfaces along the x direction against dimerization.[30, 31]

Increasing interchain coupling J_x , the model will be brought into a Néel phase. The quantum critical point between the SPT Haldane and the Néel phase [30, 32–37] locates at $J_x = 0.043648(8)$ and the transition belongs to the 3D O(3) universality class. [36]

To study the SCBs of the model, we use periodic boundary condition along one direction and make open boundary boundaries along the other direction by cutting a row/column of bonds perpendicular to this direction. The spins connected by these bonds form two surfaces. Figure 1(a) shows a system with periodic boundary in the x direction and open boundaries in the y direction. Two x surfaces are formed by cutting a row of J_y bonds. Figure 1(b) shows a system with periodic boundary in the y direction and open boundaries in the x direction. In this case, two y surfaces are exposed.

The model is suitable for checking the role of the symmetry-protected gapless surface state in inducing the special SCB, because, different from previous works [7, 11], there's no dimerization, therefore, no dangling or non-dangling surface. Using unbiased quantum Monte Carlo (QMC) simulations, we find that, in the gapped Haldane phase, the string order parameter \mathcal{S} of the chain, either with open ends or periodic, decays exponentially with system size L . This is different from simulation results reported in [30], but in agreement with the theoretical prediction[29]. The spin-spin correlation along the surface decays algebraically for the x surfaces, but exponentially for the y surfaces. This is attributed to the fact that, in the SPT phase, the latter surfaces (y surfaces) are gapped, while the former surfaces are gapless, because a spin-1 model can has spin-1/2 excitations. Furthermore, we find out that the system with x surfaces shows special SCB, while the system with y surfaces shows ordinary SCB. This proves that the nontrivial surface states of a SPT state can induce nonordinary SCB.

The paper is organized as follows: In Sec. II, we introduce the model, discuss the bulk quantum phase transition and describe the quantum Monte Carlo methods. In Sec. III, we study the properties of the SPT phase. We investigate the string order parameter and its decaying behavior when couplings among chains are included. In

particular, we discuss the string order parameter in the case that surfaces are presented. We also show the surfaces are gapless when the bulk are gapped in the SPT phase. We then discuss the SCBs at bulk critical point in Sec. IV. In subsection IV A, we present our results on the ordinary transition along x surfaces. In subsection IV B, the results of special SCB are presented. We conclude in Sec. V.

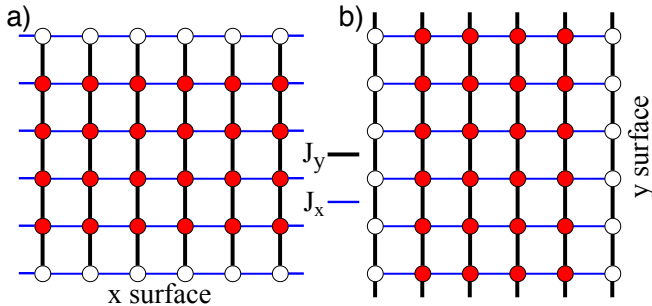


FIG. 1. The coupled $S = 1$ vertical Haldane chains form 2D square lattice with two different settings of boundaries. (a) periodic boundary condition are applied in the x direction while open boundaries in the y direction. Two surfaces along the x direction are exposed. (b) periodic boundary condition are applied in the y direction while open boundaries are used in the x direction. Two y surfaces are formed. J_x (horizontal blue bonds) and J_y (vertical bold black bonds) are inter-chain and intra-chain couplings, respectively.

II. MODELS AND METHOD

The model we study here is $S = 1$ AFH chains (Haldane chains) coupled by weak interchain interactions, forming a 2D square lattice, as illustrated in Fig. 1. The Hamiltonian of the model is given by

$$H = J_x \sum_{\langle i,j \rangle_x} \mathbf{S}_i \cdot \mathbf{S}_j + J_y \sum_{\langle i,j \rangle_y} \mathbf{S}_i \cdot \mathbf{S}_j, \quad (1)$$

where $\langle i,j \rangle_y$ are nearest neighbors along the chains with the coupling strength $J_y > 0$, while $\langle i,j \rangle_x$ are nearest neighbors in two neighboring chains, with the interchains coupling $J_x > 0$. We set $J_y = 1$ and consider $g \equiv J_x < J_y$. The system has a quantum critical point (QCP) separating the Haldane phase and the Néel phase at $g_c = (J_x)_c = 0.043648(8)$. [36] The transition belongs to the 3D classical $O(3)$ universality class with the correlation exponent ν estimated to be 0.70(1) and $\gamma = 1.373(3)$. [36]

For $0 < g < g_c$, the bulk is at a gapped disordered Haldane phase, which is a SPT phase [30] with y -parallel Haldane chains behaving as independent $S = 1$ AFH chains. However, the string order parameter is zero, because the string order is unstable under the perturbation of interchain couplings [29]. Cutting the lattice along the x direction, each independent $S = 1$ Haldane chain

carries two effectively degenerate $S = 1/2$ spins at the ends, which form the x surfaces of the system. These effective spins couple each other on the edge along the x direction by weak interchain couplings, forming two gapless $S = 1/2$ AFH chains. On the other hand, cutting along the y direction exposes two surfaces formed by two periodic $S = 1$ Haldane chains, thus does not introduce gapless edge states. The two different cuts are graphed in Fig. 1.

In this work, we use the Stochastic Series Expansion (SSE) [38] quantum Monte Carlo (QMC) method with the directed loop updating algorithm [39] to study the system, with special attention put on the SPT phase and the surface critical behavior induced by the SPT physics and bulk critical mode. The simulations are performed on square lattices. To avoid large corrections to scaling due to the strong spatial anisotropy in the couplings [36], we set aspect ratio $R = L_y/L_x = 4$ where L_x and L_y is the linear size in the x and y direction, respectively. Henceforth, we use $L = L_y$ as the linear size of the system. The inverse temperature β is scaled as L to probe ground state properties, considering the dynamical critical exponent $z = 1$ for the bulk criticality.

III. SYMMETRY PROTECTED TOPOLOGICAL PHASE

In 1D, the Haldane phase is characterized by the hidden nonlocal string order [28], which is defined as follows

$$\mathcal{S}(i, j) = \langle S_i^z \exp(i\pi \sum_{k=i+1}^{j-1} S_k^z) S_j^z \rangle \quad (2)$$

where i, j are two spins in the chain and k labels a spin in between of them. The string order is finite for $|i-j| \rightarrow \infty$ in the 1D Haldane phase. This definition can also be used for the 2D spin-1 AFH system by restricting i, j and k as spins along an individual chain.

It was predicted that the string order is not stable and decays exponentially for arbitrarily weak interchain coupling by means of perturbation theory and bosonization [29]. However, it was shown numerically that the string order parameter decays algebraically in the Haldane phase of coupled Haldane chains according to finite-size data up to linear size $L = 72$ at interchain couplings much weaker than critical value. [30] Therefore it is necessary to investigate the string order parameter for various values of $g < g_c$ in the Haldane phase, including those that are close to the critical point. We will calculate the parameter up to much larger system sizes than those reached in the literature, so that we can pin down the scaling behavior of the string order parameter in the 2D Haldane phase. Besides, we will investigate the string order parameter in different boundary conditions.

We focus on the string order parameter $\mathcal{S}(L/2)$ at the maximum available distance $|i-j| = L/2$ of a chain along y direction. The results are shown in Fig. 2.

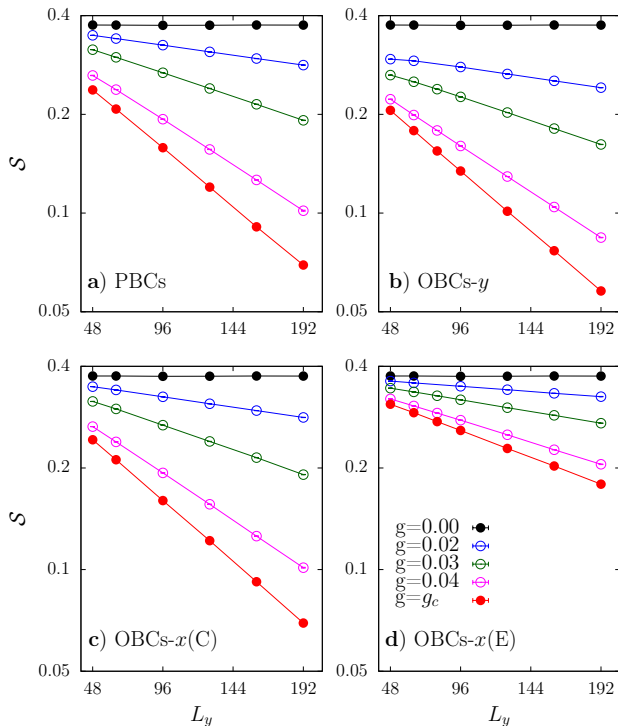


FIG. 2. String order parameter of a chain at the maximum available distance $\mathcal{S}(L/2)$ at different interchain couplings for systems with (a) periodic boundaries, (b) open boundaries in the y direction, and (c)(d) open boundaries in the x direction, shown on a linear-log scale. For (b), the chain has open ends at the x surfaces where the starting spin locates. For (c) the chain is at the center of the system, and, for (d), the chain is one of the y surfaces.

For systems with periodic boundary conditions (PBCs) in both x and y directions, the results are shown in Fig. 2(a). We find that, for $g < g_c$, the nonlocal string order decays exponentially with system size as it is large enough, in agreement with the theoretical prediction of 29. For small g , e.g., $g = 0.01$, which is studied in 30, such exponentially decaying behavior are clearly seen only when system sizes are much larger than 72.

We then study the nonlocal string order parameter for systems with periodic boundary condition along one direction, but open boundary condition along the other direction with two surfaces exposed, as shown in Fig. 1. For the configuration Fig. 1(a), we calculate $\mathcal{S}(L/2)$ along a chain connecting the two x surfaces. The starting site in Eq. (2) is chosen to be at the surface and the ending site sits at the center of the chain. The results are shown in Fig. 2(b). The nonlocal string order parameter is found decaying exponentially with system size L . For the configuration Fig. 1(b), we study two situations. First, we calculate the string order parameter $\mathcal{S}(L/2)$ of the periodic chain forming the y surface. The results are shown in Fig. 2(d); Then we calculate $\mathcal{S}(L/2)$ of the chain sitting at the middle of the system. The results

are shown in Fig. 2(c). Again, we see exponential decay of the string order parameter. Apparently, the open boundaries do not affect much the finite-size behavior of the nonlocal string order, which remains fragile as in periodic systems.

The exponentially decaying of the string order parameter is expected to behave in the following way

$$\mathcal{S}(L/2) \propto \exp(-\alpha L/2), \quad (3)$$

with $\alpha \sim g^2$ in the case of g being small enough.[29] Similar to correlation functions, α could be regarded as the inverse characteristic length. We fit $\mathcal{S}(L/2)$ of systems with all boundary conditions at several values of g below g_c to Eq.(3). The fits are carried out with data up to system size $L = 192$. To obtain statistically sound fits, small systems with $L < 48$ are excluded. The obtained α as functions of g^2 for different boundary conditions are graphed in Fig. 3. We then fit the estimated $\alpha(g)$ for various boundary conditions to the function $\alpha = cg^2$ with c an unknown parameter. We find perfectly consistency to the theory for $g \leq 0.03$, as illustrated in Fig. 3.

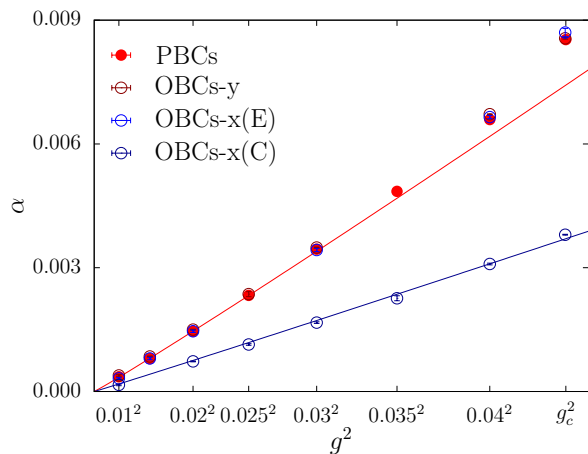


FIG. 3. The inverse characteristic length α versus g^2 for systems with different boundary conditions. The two straight lines correspond to the scaling of the form $\alpha(g) \propto g^2$.

Nonetheless the string order parameter vanishes in 2D, the Haldane phase remains a gapped weak SPT phase[30], which is fabricated by alignment of 1D SPT state. The 1D Haldane chain with open ends supports degenerate $S = 1/2$ edge states. In 2D, we expect the open ends forming two surfaces which can be considered as two gapless $S = 1/2$ AFH chains, as shown in fig. 1(a), while the bulk ground state is gapped. These gapless states are protected by the translational symmetry along the x direction.[40]

To show the above expectations are correct, we study the equal-time spin-spin correlation defined as

$$C(i, j) = \langle (S_i^x S_j^x + S_i^y S_j^y) \rangle \quad (4)$$

that equals to $2\langle S_i^z S_j^z \rangle$ by symmetry and can be calcu-

lated through the following Green function

$$G(i, j) = \frac{1}{2} (\langle S_i^+ S_j^- \rangle + \langle S_i^- S_j^+ \rangle), \quad (5)$$

which can be measured efficiently with improved estimator by using the loop updating algorithm in the SSE QMC simulations.[41]

We focus on two specific correlations. One is $C_{\parallel}(L_{\alpha}/2)$ that averages $C(i, j)$ between two surface spins i and j at a distance $L_{\alpha}/2$ over the $\alpha = x$ or y surface under consideration. The other is $C_{\perp}(L_{\alpha}/2)$ that averages $C(i, j)$ between two spins i and j at a distance $L_{\alpha}/2$ with i fixed on the surface and the other spin j located at the center of the bulk, with the direction i to j perpendicular to the surface, along the α direction.

We first study the system with x surfaces. The results of $C_{\parallel}(L_x/2)$ at several $g \leq g_c$ as functions of system size L_x are plotted on a log-log scale in Fig. 4(a). We find that $C_{\parallel}(L_x/2)$ decays algebraically with (large enough) system size L for all g , including the critical g_c , indicating that the surface state is gapless, or critical. This is further manifested by the inset in which the correlations are plotted on a linear-log scale.

More precisely, we expect the following finite-size scaling ansatz for C_{\parallel}

$$C_{\parallel}(L/2) = L^{-(d+z-2+\eta_{\parallel}(g))} (a + bL^{-\omega}), \quad (6)$$

where $\eta_{\parallel}(g)$ is the surface anomalous dimensions, which depends on g . $\omega > 0$ is the effective exponents controlling corrections to scaling. $d + z$ is the space-time dimension. In the present model, $d = 2$ and $z = 1$.

The largest system size we reached is $L_y = 320$ and $L_x = 80$. By excluding small system sizes gradually, we can obtain statistically sound fits of Eq.(6) for all g , with the correction to scaling term removed. For example, for the case $g = 0.03$, we find $1 + \eta_{\parallel} = 1.82(3)$ by fitting Eq.(6) with the correction to scaling term discarded to the finite-size data in the range of $48 \leq L_x \leq 80$. The reduced χ^2 of the fit is 1.58 with the goodness of fit defined as the P-value of the χ^2 distribution $P = 0.175$. For $g = 0.02$, we have to exclude sizes smaller than $L_x = 32$ to obtain satisfying fit. We have also tried to include multiplicative logarithmic correction to the simple power law decay as in the 1D spin-1/2 AFH chain, but no improving was found in the fitting, and the decay exponents $1 + \eta_{\parallel}$ are always close to 2. We conclude that, although the edge is gapless, the anomalous exponent is not consistent with the $1/r$ decay with multiplicative logarithmic corrections for the spin-1/2 AFH chain. [42–44] For comparison, $C_{\parallel}(L/2)$ for the $S = 1/2$ AFH chain is shown in Fig. 4(a). It is evident that the x surface can not be considered as a spin-1/2 AFH chain naively.

Meanwhile, as shown in Fig. 4(b) on a linear-log scale, $C_{\perp}(L_y/2)$ exponentially decays with system size L_y at all $g < g_c$, indicating that the bulk is gapped for $g < g_c$. This is further exhibited by the log-log plot in the inset. For $g = 0.03$, a fit to the function $C_{\perp}(x) = a \exp(-x/\xi)$

with finite-size data in the range $128 \leq L_y \leq 320$ finds statistical sound results $\xi = 27.8(1)$, with reduced $\chi^2 = 1.25$ and the P-value $P = 0.28$.

On the other hand, for the system with open surfaces along y direction, exposed by cutting a column of interchain J_x bonds, the surfaces are two periodic spin-1 chains weakly coupled to the bulk, as illustrated in Fig. 1(b). We find that the surface states is gapped, even though the string order parameter vanishes with finite interchain coupling included. This is obtained from the results of $C_{\parallel}(L_y/2)$ at several g as functions of system size L_y , as shown in Fig. 5(a). Although there are strong finite-size effects, we can fit $C_{\parallel}(L_y/2)$ to exponentially decaying forms of system size L_y for large enough system sizes, which indicates the surface states are gapped at the Haldane phase. Meanwhile, as shown in Fig.5(b), $C_{\perp}(L_x/2)$ also exponentially decay with system size L_x at $g < g_c$, reflecting the fact that the bulk is gapped for $g < g_c$.

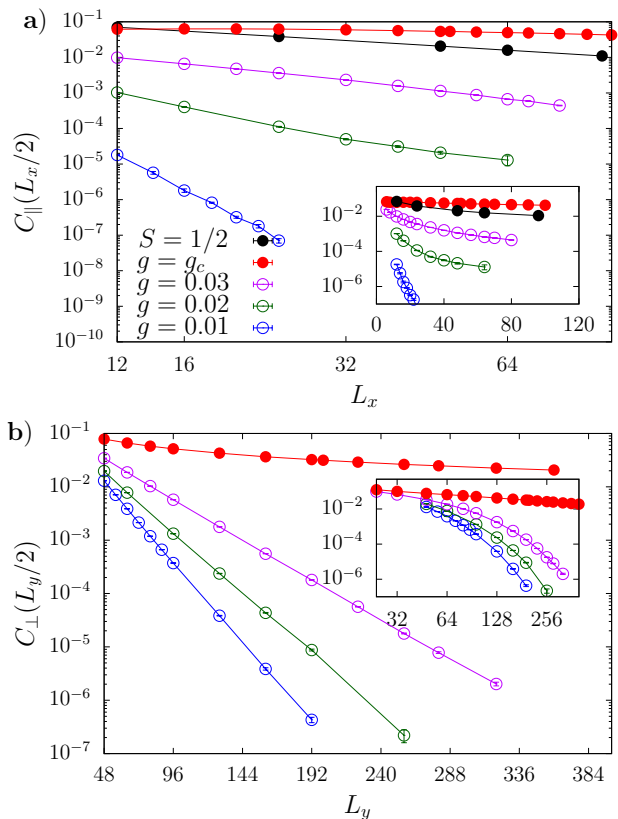


FIG. 4. Correlation functions $C_{\parallel}(L_x/2)$ (a) and $C_{\perp}(L_y/2)$ (b) of the systems with x surfaces, as illustrated by Fig. 1(a), at the SPT phase with different g up to g_c . For the purpose of comparison, $C_{\parallel}(L/2)$ for the $S = 1/2$ AFH chain is also shown here. (a) The main plot is set on a log-log scale, the inset is on a linear-log scale. (b) The main plot is on a linear-log scale and the inset is on a log-log scale.

IV. SURFACE CRITICAL BEHAVIORS

At bulk critical point, some classical systems can have ordered surface if the interactions at the surface are enhanced. When this happens, the ordered surface exhibits additional singular behavior, which is called as an extraordinary transition. Furthermore fine-tune the surface couplings can lead the surface to a multicritical point, at which surface and bulk are critical simultaneously. This is the special transition. As discussed in Sec. I, according to quantum-classical corresponding, we expect no special and/or extraordinary surface transition in the present model, because there can not be a long-range order that breaks the continuous symmetry in 2D surface of a classical model at finite temperature due to Mermin-Wagner theorem.[4] Here in this section, we show that, due to pure quantum effect, special surface transition can be realized at the surface perpendicular to the coupled Haldane chains without fine-tune surface couplings, while at another surface, the system shows the ordinary SCB.

To study the surface critical behavior, we here, besides the correlations C_{\parallel} and C_{\perp} , introduce the squared staggered surface magnetization defined as

$$m_{s1}^2 = \frac{1}{2L_{\alpha}^2} [\langle (\sum_{i \in \text{surface}} (-1)^i S_i^x)^2 \rangle + \langle (\sum_{i \in \text{surface}} (-1)^i S_i^y)^2 \rangle], \quad (7)$$

with i labeling spins on the surface, which equals to $\frac{1}{L_{\alpha}^2} \langle (\sum_{i \in \text{surface}} (-1)^i S_i^z)^2 \rangle$ by symmetry. m_{s1}^2 can be expressed with the Green function defined in Eq.(5)

$$m_{s1}^2 = \frac{1}{L_{\alpha}^2} \sum_{i,j \in \text{surface}} (-1)^{i+j} G(i,j), \quad (8)$$

with i, j the spins on the surface and $\alpha = x$ for the surface along x-direction and $\alpha = y$ for the y surface, respectively.

At bulk QCP, the surface should show power law surface critical behaviors. Besides the Eq. (6) with $\eta_{\parallel} = \eta_{\parallel}(g_c)$, $m_{s1}^2(L)$ and $C_{\perp}(L)$ obey the following finite-size scaling forms [2]

$$m_{s1}^2 L = c + L^{2y_{h1} - (d+z)}(a + bL^{-\omega}), \quad (9)$$

and

$$C_{\perp}(L) = L^{-(d+z-2+\eta_{\perp})}(a + bL^{-\omega}). \quad (10)$$

in which y_{h1} is the scaling dimension of the surface staggered magnetic field h_1 , η_{\parallel} and η_{\perp} are two surface anomalous dimensions. The constant c in Eq. (9) results from the short-range nonuniversal part of m_{s1}^2 . $\omega > 0$ is the effective exponents controlling corrections to scaling. $d+z$ is the space-time dimension. In the present model, $d = 2$ and $z = 1$.

The surface critical exponents y_{h1} , η_{\parallel} and η_{\perp} are expected to satisfy the following scaling relations[3, 45, 46]

$$2\eta_{\perp} = \eta_{\parallel} + \eta \quad (11)$$

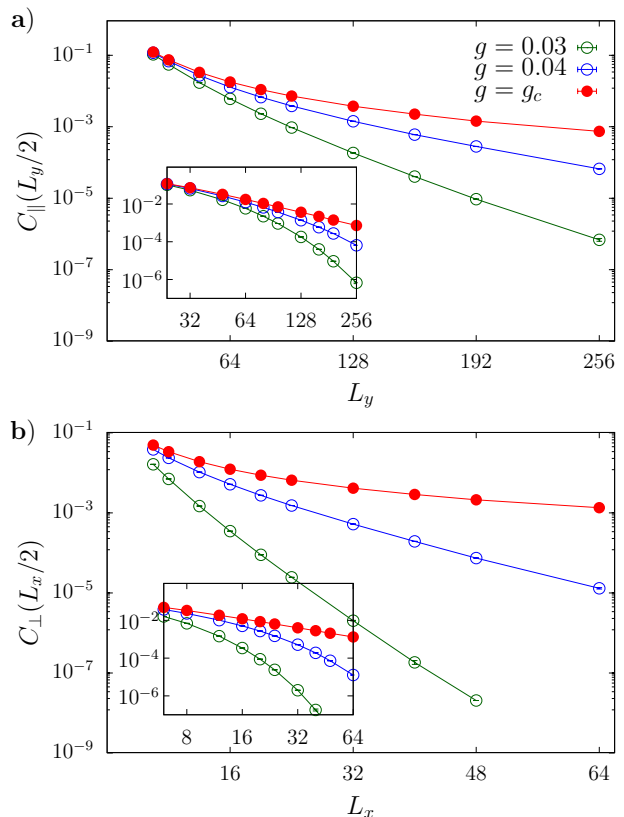


FIG. 5. For system with surfaces shown in Fig. 1(b) at the SPT phase with different g up to g_c , (a) correlation along the surface $C_{\parallel}(L_y/2)$ vs L_y , (b) correlation perpendicular to the surface $C_{\perp}(L_x/2)$ vs L_x . The two main plots are set on linear-log scales and the two insets are on log-log scales.

and

$$\eta_{\parallel} = d + z - 2y_{h1}, \quad (12)$$

with η the anomalous magnetic scaling dimension of the bulk transition in the $d+z$ spacetime. For our model, $d+z = 3$ and $\eta = 0.0357(13)$ [47] is the anomalous magnetic scaling dimension for the 3D O(3) universality class.

We now proceed to study systems with surfaces at its bulk quantum critical point to explore the surface critical behaviors.

A. Ordinary transition

We first consider the system that is cut to expose two y surfaces along the y direction, see Fig. 1(b). The surfaces are periodic spin-1 chains with length L_y . To study the SCB of such a system at the bulk quantum critical point, the staggered surface magnetization m_{s1}^2 , spin correlations $C_{\parallel}(L_y/2)$ and $C_{\perp}(L_x/2)$ are calculated at g_c . The numerical results of C_{\parallel} and C_{\perp} are graphed in Fig. 5 and the results of rescaled m_{s1}^2 are plotted in Fig. 6(b).

The spin correlations $C_{\parallel}(L_y/2)$ and $C_{\perp}(L_x/2)$ decay algebraically, as can be seen in the insets of Fig. 5. This is different from the behaviors in the SPT Haldane phase, where both of them decay exponentially. We fit the data to finite-size scaling Eq. (6) and (10) to find the anomalous surface scaling dimensions η_{\parallel} and η_{\perp} .

For large enough systems, the correction to scaling terms in Eq. (6) and (10) can be neglected. To estimate η_{\parallel} , we found the fit of $C_{\parallel}(L_y/2)$ is statistically sound for system sizes $L_y \geq 128$ and obtained $\eta_{\parallel} = 1.38(2)$. Using data of system sizes $L_x \geq 48$, we found statistically sound fit of $C_{\perp}(L_x/2)$ and obtained $\eta_{\perp} = 0.68(1)$.

To fit for more system sizes, we need to include the correction to scaling terms in Eq.(6) and (10). However, it's hard to estimate the value of the effective exponent ω . To verify our fits of η_{\perp} and η_{\parallel} , we define an effective exponent $\hat{\eta}$ for a pair of systems with sizes L and $2L$,

$$\hat{\eta}(L) = \frac{1}{\ln(2)}(\ln C(2L) - \ln C(L)), \quad (13)$$

where $C(L)$ stands for one of the two correlations $C_{\parallel}(L_y)$ or $C_{\perp}(L_x)$. According to Eq.(6) and (10), $\hat{\eta}(L)$ should converge to $1 + \eta$ in the following way

$$\hat{\eta}(L) = 1 + \eta + cL^{-\omega}, \quad (14)$$

where η stands for η_{\parallel} or η_{\perp} for corresponding $\hat{\eta}$.

As shown in Fig. 6(a), the two effective exponents converge to the $1 + \eta_{\parallel}$ and $1 + \eta_{\perp}$, respectively. Fitting the data to Eq. (14), we obtained statistically sound fits for data of sizes $L \geq 24$. The final estimations are $\eta_{\parallel} = 1.378(9)$ with $\omega = 1.45(4)$ and $\eta_{\perp} = 0.69(2)$ with $\omega = 0.99(5)$. The results are in good agreement with the estimations of η_{\parallel} and η_{\perp} obtained above. The final estimations are listed in Tab. I.

The rescaled surface magnetization $m_{s1}^2 L_y$ as function of system size L_y exhibits a power-law decay to a nonzero constant c , in the way of Eq. (9). For large enough system sizes, the correction to scaling with effective exponent ω in Eq. (9) can be dropped. A nonlinear fit based on Eq. (9) finds $c = 4.552(1)$, suggesting that the transition is of ordinary type. The scaling dimension of the surface magnetic field is obtained as $y_{h1} = 0.78(1)$. In the fit, we restricted the system sizes to $L_y \geq 64$ and, thus, neglected the correction to scaling term. We have also tried to set $\omega = 1.5$ in Eq. (9) and fitted it to data of sizes $L_y \geq 24$. The fit has good reduced $\chi^2 = 1.18$ and p-value $P = 0.31$, and finds $c = 4.554(1)$ and $y_{h1} = 0.79(1)$, which are consistent well with the fit without correction to scaling term but only for large enough system sizes. The final estimate of y_{h1} is listed in Tab. I.

The exponents found here obey the scaling relations Eqs. (11) and (12). They also agree well with the corresponding exponents found for the ordinary surface transition of O(3) bulk criticality in other 2D quantum models [7, 10–12], and are consistent with those of the ordinary transition of the 3D classical O(3) universality class [48].

This is understandable, because we know that, for the ordinary SCBs, the algebraic correlations are all bulk-induced behaviors. This is true also for quantum critical system so far discussed. However, all those ordinary SCBs found thus far in the quantum critical points of dimerized systems happen at surfaces formed by so called *non-dangling* spins. But here, the interesting thing is that the y surface of the current model are weakly coupled to the bulk, therefore, are actually formed by kind of *dangling* spins.

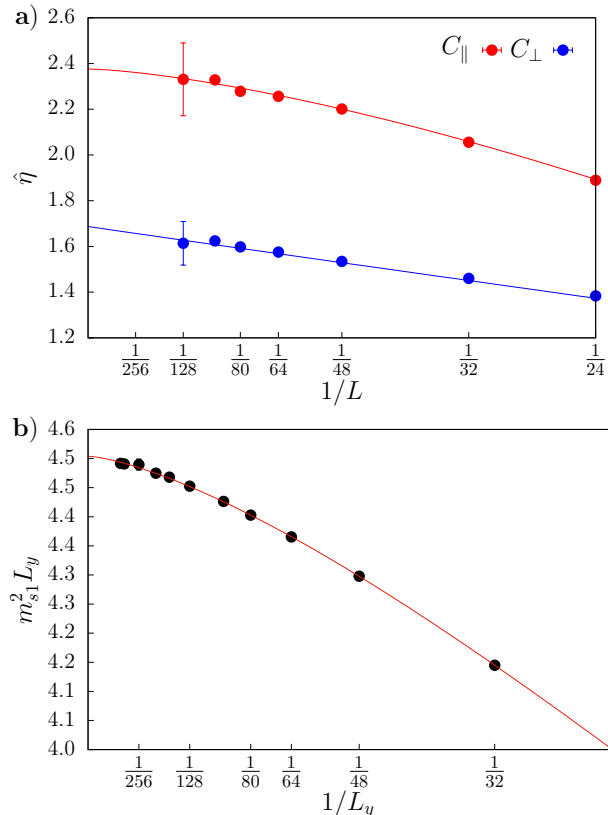


FIG. 6. Ordinary surface transition of the system configuration Fig. 1(b). (a) Finite-size dependence of effective surface anonymous exponents $\hat{\eta}(L)$ for C_{\perp} (blue symbols) and C_{\parallel} (red symbols). The lines show fits giving the estimates of η_{\perp} and η_{\parallel} , respectively. (b) The rescaled squared staggered magnetization of the surface spins $m_{s1}^2 L_y$. The curve is a fit to the expected power law decay with a constant included.

B. Special transition

We now study the critical behavior of the surfaces along the x direction exposed by cutting a row of J_y bonds, as illustrated by Fig. 1(a). In Sec. III we have shown that the surface state of the x surface is gapless even in the quantum disordered SPT phase. Together with the gapless critical mode induced by the critical bulk, a special SCB is expected. We calculate the surface magnetization $m_{s1}^2(L_x)$, the spin correlations $C_{\parallel}(L_x/2)$

TABLE I. Results of Surface critical exponents of the coupled Haldane chains(CHC). For the convenience of the readers, results of the SCBs on other models with transitions in the 3D O(3) universality class are also listed for comparison, with CD-DAF the Dimer-AF QCP of the columnar dimerized Heisenberg model, SD-DAF the Dimer-AF QCP of the staggered dimerized Heisenberg models, DS-DAF the Dimer-AF QCP of the dimerized Heisenberg model on the DS lattice; DS-PAF the PVBC-AF QCP of dimerized Heisenberg model on the DS lattice, 3D CH the three-dimensional classical Heisenberg model. For the types of cuts, D means dangling and N means nondangling. The field theoretical results(FT) from various methods are also listed for comparison.

SCB class	Model/methods	cuts	Spin S	η_{\parallel}	η_{\perp}	y_{h1}
Sp. Ord.	CHC	x surface y surface	1 1	-0.57(2) 1.38(2)	-0.27(2) 0.69(2)	1.760(3) 0.79(2)
Sp. [10]	CD-DAF	D	1/2	-0.445(15)	-0.218(8)	1.7339(12)
Sp. [11]		D	1/2	-0.50(6)	-0.27(1)	1.740(4)
Sp. [12]		D	1	-0.539(6)	-0.25(1)	1.762(3)
Ord. [11]		N	1/2	1.30(2)	0.69(4)	0.84(1)
Ord. [10]		N	1/2	1.387(4)	0.67(6)	0.840(17)
Ord. [12]		N	1	1.32(2)	0.70(2)	0.80(1)
Ord. [10]	SD-DAF	N	1/2	1.340(21)	0.682(2)	0.830(11)
Sp. [7]	DS-DAF	D	1/2	-0.449(5)	-0.2090(15)	1.7276(14)
Sp. [11]		D	1/2	-0.50(1)	-0.228(5)	1.728(2)
Ord. [11]		N	1/2	1.29(6)	0.65(3)	0.832(8)
Ord. [7]	DS-PAF	N	1/2	1.327(25)	0.680(8)	0.810(20)
Ord. [11]		N	1/2	1.33(4)	0.65(2)	0.82(2)
Sp. [11]		D	1/2	-0.517(4)	-0.252(5)	1.742(1)
Ord. [48]	3D CH		class.			0.813(2)
Ord. [49]	FT, 4-d ϵ -exp		class.	1.307	0.664	0.846
Ord. [50]	FT, d-2 ϵ -exp		class.	1.39(2)		
Ord. [51, 52]	FT, Massive field		class.	1.338	0.685	0.831
Ord. [53]	FT, Conformal bootstrap		class.			0.831
Sp. [54]	FT, 4-d ϵ -exp		class.	-0.445	-0.212	1.723

and $C_{\perp}(L_y/2)$ for systems with x surfaces at the bulk critical point g_c .

The numerical results of $C_{\parallel}(L_x/2)$ and $C_{\perp}(L_y/2)$ as functions of system size are shown in Fig. 4. Power-law decay of $C_{\parallel}(L_x/2)$ and $C_{\perp}(L_y/2)$ with system size $L_x(L_y)$ are observed.

We now apply finite-size scaling analysis to find out the surface anomalous exponents.

We start with fitting the scaling ansatz Eq. (10) to the finite-size data of $C_{\perp}(L_y/2)$. First we only use data of large enough system sizes, expecting the correction to scaling term can be discarded. This is true for $L \geq 200$, we find that there's no need to include the correction term in Eq. (10). Our fit finds a statistically sound estimate of $\eta_{\perp} = -0.27(1)$. The result is also stable upon further excluding data points of small sizes. Still, it's tempting to include the correction to scaling term, so that we can fit more data of smaller sizes. However, it's hard to find the value of the effective exponent ω . Setting ω to different values, e.g., $\omega = 1$ or 1.5, leads different estimates of η_{\perp} .

We then define an effective exponent $\hat{\eta}$ for a pair of systems with sizes L and $2L$ as in Eq. (13), with $C(L)$ stands for correlations C_{\perp} . $\hat{\eta}(L)$ should converge to $1 + \eta_{\perp}$ in the way of Eq. (14), according to Eq.(10). We show the size dependence of the effective exponent $\hat{\eta}$ in Fig. 7(a) and fit the data to Eq. (14). We find statistically sound estimate of $\eta_{\perp} = -0.27(2)$ for data of $L \geq 64$, with

the effective correction exponent found to be $\omega = 1.7(5)$. This value of ω is different from that in other models studied thus far [7, 10–12], where ω is found (or simply set) to be 1. The obtained results of η_{\perp} are listed in Tab. I.

The rescaled surface magnetization $m_{s1}^2 L_x$ as function of system size L_x are graphed on a log-log scale in Fig. 7(b), showing a power-law behavior, as expected in Eq. (9) with the constant $c = 0$. Using data of system sizes larger than $L = 200$, we obtain statistically sound fit to Eq. (9) with the correction to scaling term discarded, since the system sizes are sufficiently large. The fit leads to $y_{h1} = 1.761(2)$. The result is stable upon further excluding more data points. If we include the correction to scaling term, we can fit more data of smaller sizes to the scaling form Eq.(9). In this case the fitting results are not sensitive to the value of ω used. Statistically consistent estimates of y_{h1} are obtained. The best fit is $y_{h1} = 1.758(2)$ with $\omega = 1.5$ for data of $L \geq 128$. The final estimate is listed in Tab. I.

We now turn to fit the data of C_{\parallel} to the scaling ansatz Eq. (6). First we only use data of large enough system sizes, expecting the correction to scaling term can be discarded. With data of $L \geq 256$, this leads to $\eta_{\parallel} = -0.67(2)$. However, further discarding small system sizes leads to changing of the estimate of η_{\parallel} . This suggests that the correction to scaling term can not be dropped even for sizes larger than 256.

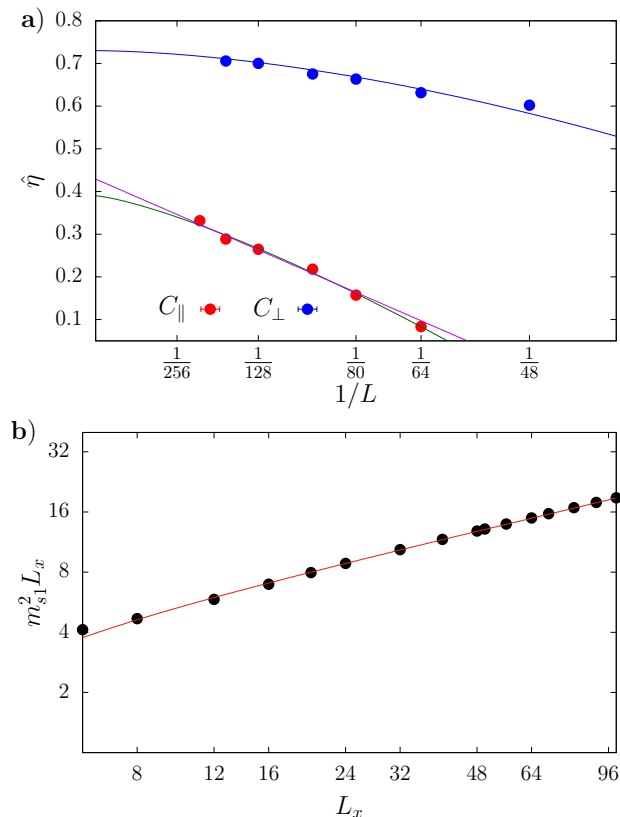


FIG. 7. Non-ordinary surface transition on the surfaces of the configuration Fig. 1(a). (a) Finite-size dependence of the effective surface anomalous exponent $\hat{\eta}(L)$ for C_{\perp} (blue symbols) and C_{\parallel} (red symbols). The blue line shows a fit to $\hat{\eta}$ of C_{\perp} . The red and dark-green lines show two fits to $\hat{\eta}$ of C_{\parallel} . (b) The rescaled squared magnetization of surface spins $m_{s_1}^2 L_x$. The curve is a fit to the expected scaling.

We thus include the correction term with ω setting to 1 and 1.5, respectively, in Eq. (6) and fit the data to it. We can obtain statistically sound fits for data of system size $L \geq 160$ for both values of ω . However, the obtained η_{\parallel} are different and still flow with the ranges of the system sizes used in the fits.

We then define an effective exponent $\hat{\eta}$ for a pair of systems with sizes L and $2L$ as in Eq. (13), with $C(L)$ stands for correlations C_{\parallel} . According to Eq.(6), $\hat{\eta}(L)$ should converge to $1 + \eta_{\parallel}$ in the way of Eq. (14). The size dependent effective exponent $\hat{\eta}$ are graphed in Fig. 7(a). Fitting the data to Eq. (14), we find statistically sound estimate of $\eta_{\parallel} = -0.61(3)$ for data of $L \geq 64$, with the effective correction exponent $\omega = 1.3(2)$. This fit is shown as the dark-green line in Fig. 7(a). The value of ω is slightly different from 1 that was assumed in other models studied thus far[7, 10–12]. However, if we fixed $\omega = 1$ and restricted to system sizes $L \geq 100$, we find $\eta_{\parallel} = -0.57(2)$ with reduced $\chi^2 = 2.5$ and P-value $P = 0.11$. The fit is shown as the red line in Fig. 7(a). This last estimate of η_{\parallel} obey the scaling relations Eqs. (11) and (12) with other exponents obtained

above. It also agrees with or is close to results found at the dangling surfaces of other models with dimerized Hamiltonian[10–12], where gapless surface state and the bulk critical state coexists, and the multicritical point is named special transition or nonordinary transition. We therefore choose this value as the final estimate, which is listed in Tab. I.

It was first noticed by Ding et al [10] that the exponents found in the nonordinary transitions mentioned above agree surprisingly to the field theoretic prediction with ϵ expansion ($\epsilon = 4 - d$) to the special SCB of d -dimensional $O(n)$ models by setting $\epsilon = 1$ and $n = 3$, [3, 54] even though the 3D $O(3)$ model does not feature such a multicritical point, as discussed in Sec. I. However, such SCB was claimed less universal because of slightly variation when perturbing the surface. [11, 12]

Although a previous work attributes the phenomena to the gapless surface state of the SPT bulk state [7], the role of SPT was challenged by the fact that the non-dangling edge shows ordinary SCB at the same AKLT to Néel QCP. It was further opposed by the finding that the suggested AKLT state is not a real SPT phase. [11] Our model shows a genuine SPT phase separated from the Néel phase by a QCP in the 3D $O(3)$ universality class. Our results provide evidences of nonordinary SCB induced by SPT physics in the surface perpendicular to the spin-1 chains. In particular, our model does not have a dangling edge or surface, instead, the surface we study here is not dangling at all, still we find the nonordinary SCBs at the bulk 3D $O(3)$ critical point. We therefore believe the SPT physics is essential here.

V. CONCLUSIONS

The discovery of nonordinary surface transitions at bulk quantum critical point, that is precluded in corresponding classical critical point, has inspired interests in the investigations on the quantum origin of such behaviors. So far researches were focused on dimerized anti-ferromagnetic Heisenberg models and it was noticed that surfaces formed by dangling spins in the dimerized models show such nonordinary SCBs. However, the role of SPT and spin-1/2 related topological terms were still under debate.

We have studied the system of coupled Haldane chains in two-dimensional square lattice with interchain couplings, which has an SPT Haldane phase when the interchain couplings are weak. Increasing interchain couplings, the model enters a Néel phase through a quantum critical point belonging to the 3D $O(3)$ universality class. Different from previously studied dimerized models, this model does not have surfaces formed by dangling or non-dangling spins, therefore offers an opportunity to test the role of SPT in the origin of nonordinary SCBs. In particular, the model is anisotropic. The surfaces along the spin-1 chain direction (x surfaces) are completely different from the surfaces perpendicular (y surfaces) to the

chain direction.

Using unbiased quantum Monte Carlo simulations, we have studied in a great detail the string order parameter of the gapped Haldane phase and its surface states. We found that, although the string order decay exponentially with system size, as interchain interactions are introduced, the x surface states are gapless even in the gapped Haldane phase while the y surface is gapped. This verified that the gapless surface state is the property of a SPT phase.

We have then studied the surface critical behaviors of surfaces along the x and the y direction at the bulk critical point, by calculating the spin-spin correlations along the surface and/or perpendicular to the surface and the surface magnetization. Ordinary SCBs were found at the surfaces along the spin-1 chain direction, which have gapped surface states in the gapped SPT phase. We found that gapless surface states at the surfaces perpendicular to the spin-1 chains in the gapped SPT phase result in multicritical special transitions at the quantum critical point, with exponents in agreement with those found in other SCBs at dangling surfaces of dimerized models. This behavior is of pure quantum origin, because nonordinary SCB is precluded in the 3D classical $O(3)$

models. All exponents found in the surface transitions, either ordinary or special, satisfy the scaling relations.

Although the quantum origin of the nonordinary SCB in dimerized Heisenberg models seems not induced by the SPT physics in particular, and the mechanism of the nonordinary SCBs in these models is still not clear, our numerical results support that the SPT and its gapless surface states together with the gapless critical modes at least offers one quantum origin of nonordinary SCB.

ACKNOWLEDGMENTS

W.Z and W.G were supported by the National Natural Science Foundation of China under Grant No. 11775021 and No. 11734002. C.D. was supported by the National Natural Science Foundation of China under Grant No. 11975024 and the Anhui Provincial Supporting Program for Excellent Young Talents in Colleges and Universities under Grant No. gxyqZD2019023. L.Z. was supported by the National Natural Science Foundation of China under Grant No. 11804337 and the CAS Youth Innovation Promotion Association. The authors acknowledge supporting extended by the Super Computing Center of Beijing Normal University.

-
- [1] K. Binder, [Phase Transitions and Critical Phenomena](#), edited by C. Domb and J. L. Lebowitz, Vol. 8 (Academic Press, London, 1983).
- [2] K. Binder and P. C. Hohenberg, Surface effects on magnetic phase transitions, [Phys. Rev. B](#) **9**, 2194 (1974).
- [3] K. Binder, [Phase Transitions and Critical Phenomena](#), edited by C. Domb and J. L. Lebowitz, Vol. 10 (Academic Press, London, 1986).
- [4] N. D. Mermin and H. Wagner, Absence of ferromagnetism or antiferromagnetism in one- or two-dimensional isotropic heisenberg models, [Phys. Rev. Lett.](#) **17**, 1133 (1966).
- [5] S. Sachdev, [Quantum phase transitions](#) (Cambridge University Press, Cambridge, UK, 2011).
- [6] I. Affleck, T. Kennedy, E. H. Lieb, and H. Tasaki, Rigorous results on valence-bond ground states in antiferromagnets, [Phys. Rev. Lett.](#) **59**, 799 (1987).
- [7] L. Zhang and F. Wang, Unconventional surface critical behavior induced by a quantum phase transition from the two-dimensional affleck-kennedy-lieb-tasaki phase to a néel-ordered phase, [Phys. Rev. Lett.](#) **118**, 087201 (2017).
- [8] Z.-C. Gu and X.-G. Wen, Tensor-entanglement-filtering renormalization approach and symmetry-protected topological order, [Phys. Rev. B](#) **80**, 155131 (2009).
- [9] F. Pollmann, A. M. Turner, E. Berg, and M. Oshikawa, Entanglement spectrum of a topological phase in one dimension, [Phys. Rev. B](#) **81**, 064439 (2010).
- [10] C. Ding, L. Zhang, and W. Guo, Engineering surface critical behavior of $(2+1)$ -dimensional $o(3)$ quantum critical points, [Phys. Rev. Lett.](#) **120**, 235701 (2018).
- [11] L. Weber, F. Parisen Toldin, and S. Wessel, Nonordinary edge criticality of two-dimensional quantum critical magnets, [Phys. Rev. B](#) **98**, 140403 (2018).
- [12] L. Weber and S. Wessel, Nonordinary criticality at the edges of planar spin-1 heisenberg antiferromagnets, [Phys. Rev. B](#) **100**, 054437 (2019).
- [13] H. Mutka, C. Payen, P. Molinié, J. L. Soubeyroux, P. Colombet, and A. D. Taylor, Dynamic structure factor $[s(q,\omega)]$ of the $s=1$ quasi-one-dimensional heisenberg antiferromagnet: Neutron-scattering study on $agvp_2s_6$, [Phys. Rev. Lett.](#) **67**, 497 (1991).
- [14] T. Asano, Y. Ajiro, M. Mekata, H. Yamazaki, N. Hosoi, T. Shinjo, and H. Kikuchi, Single crystal susceptibility of the $s = 1$ one-dimensional heisenberg antiferromagnet $agvp_2s_6$, [Solid State Communications](#) **90**, 125 (1994).
- [15] Z. Honda, K. Katsumata, Y. Nishiyama, and I. Harada, Field-induced long-range ordering in an $s = 1$ quasi-one-dimensional heisenberg antiferromagnet, [Phys. Rev. B](#) **63**, 064420 (2001).
- [16] J. P. Renard, M. Verdaguer, L. P. Regnault, W. A. C. Erkelens, J. Rossat-Mignod, and W. G. Stirling, Presumption for a quantum energy gap in the quasi-one-dimensional $s = 1$ heisenberg antiferromagnet $ni(c_2h_8n_2)2no_2(clo_4)$, [Europhysics Letters \(EPL\)](#) **3**, 945 (1987).
- [17] J. P. Renard, M. Verdaguer, L. P. Regnault, W. A. C. Erkelens, J. Rossat-Mignod, J. Ribas, W. G. Stirling, and C. Vettier, Quantum energy gap in two quasi-one-dimensional $s=1$ heisenberg antiferromagnets (invited), [Journal of Applied Physics](#) **63**, 3538 (1988).
- [18] L. P. Regnault, I. Zaliznyak, J. P. Renard, and C. Vettier, Inelastic-neutron-scattering study of the spin dynamics in the haldane-gap system $ni(c_2h_8n_2)_2no_2clo_4$, [Phys. Rev. B](#) **50**, 9174 (1994).

- [19] M. Takigawa, T. Asano, Y. Ajiro, and M. Mekata, Static properties of the $s=1$ one-dimensional antiferromagnet AgVp_2S_6 , *Phys. Rev. B* **52**, R13087 (1995).
- [20] M. Takigawa, T. Asano, Y. Ajiro, M. Mekata, and Y. J. Uemura, Dynamics in the $S = 1$ one-dimensional antiferromagnet AgVp_2S_6 via ^{31}P and ^{51}V nmr, *Phys. Rev. Lett.* **76**, 2173 (1996).
- [21] I. A. Zaliznyak, D. C. Dender, C. Broholm, and D. H. Reich, Tuning the spin hamiltonian of $\text{Ni}(\text{C}_2\text{H}_8\text{N}_2)_2\text{NO}_2\text{ClO}_4$ by external pressure: A neutron-scattering study, *Phys. Rev. B* **57**, 5200 (1998).
- [22] Y. Uchiyama, Y. Sasago, I. Tsukada, K. Uchinokura, A. Zheludev, T. Hayashi, N. Miura, and P. Böni, Spin-vacancy-induced long-range order in a new haldane-gap antiferromagnet, *Phys. Rev. Lett.* **83**, 632 (1999).
- [23] B. Pahari, K. Ghoshray, R. Sarkar, B. Bandyopadhyay, and A. Ghoshray, Nmr study of ^{51}V in quasi-one-dimensional integer spin chain compound $\text{SrNi}_2\text{V}_2\text{O}_8$, *Phys. Rev. B* **73**, 012407 (2006).
- [24] V. Gadet, M. Verdager, V. Briois, A. Gleizes, J. P. Renard, P. Beauvillain, C. Chappert, T. Goto, K. Le Dang, and P. Veillet, Structural and magnetic properties of $(\text{CH}_3)_4\text{NNi}(\text{NO}_2)_3$: A haldane-gap system, *Phys. Rev. B* **44**, 705 (1991).
- [25] J. Darriet and L. Regnault, The compound $\gamma\text{-BaNiO}_5$: A new example of a haldane gap in a $s = 1$ magnetic chain, *Solid State Communications* **86**, 409 (1993).
- [26] F. D. M. Haldane, Nonlinear field theory of large-spin heisenberg antiferromagnets: Semiclassically quantized solitons of the one-dimensional easy-axis néel state, *Phys. Rev. Lett.* **50**, 1153 (1983).
- [27] I. Affleck and F. D. M. Haldane, Critical theory of quantum spin chains, *Phys. Rev. B* **36**, 5291 (1987).
- [28] M. den Nijs and K. Rommelse, Preroughening transitions in crystal surfaces and valence-bond phases in quantum spin chains, *Phys. Rev. B* **40**, 4709 (1989).
- [29] F. Anfuso and A. Rosch, Fragility of string orders, *Phys. Rev. B* **76**, 085124 (2007).
- [30] K. Wierschem and P. Sengupta, Quenching the haldane gap in spin-1 heisenberg antiferromagnets, *Phys. Rev. Lett.* **112**, 247203 (2014).
- [31] F. Pollmann, E. Berg, A. M. Turner, and M. Oshikawa, Symmetry protection of topological phases in one-dimensional quantum spin systems, *Phys. Rev. B* **85**, 075125 (2012).
- [32] S. Moukouri and E. Eidelstein, Universality class of the mott transition in two dimensions, *Phys. Rev. B* **86**, 155112 (2012).
- [33] T. Sakai and M. Takahashi, The ground state of quasi-one-dimensional heisenberg antiferromagnets, *Journal of the Physical Society of Japan* **58**, 3131 (1989).
- [34] A. Koga and N. Kawakami, Quantum phase transitions for the haldane system in higher dimensions: A mixed-spin cluster expansion approach, *Phys. Rev. B* **61**, 6133 (2000).
- [35] Y. J. Kim and R. J. Birgeneau, Monte carlo study of the $s = \frac{1}{2}$ and $s = 1$ heisenberg antiferromagnet on a spatially anisotropic square lattice, *Phys. Rev. B* **62**, 6378 (2000).
- [36] M. Matsumoto, C. Yasuda, S. Todo, and H. Takayama, Ground-state phase diagram of quantum heisenberg antiferromagnets on the anisotropic dimerized square lattice, *Phys. Rev. B* **65**, 014407 (2001).
- [37] K. Wierschem and P. Sengupta, Dimensional crossover in spin-1 heisenberg antiferromagnets: a quantum monte carlo study, *Journal of Physics: Conference Series* **400**, 032112 (2012).
- [38] A. W. Sandvik, Computational studies of quantum spin systems, *AIP Conference Proceedings* **1297**, 135 (2010).
- [39] O. F. Syljuåsen and A. W. Sandvik, Quantum monte carlo with directed loops, *Phys. Rev. E* **66**, 046701 (2002).
- [40] M. Cheng, M. Zaletel, M. Barkeshli, A. Vishwanath, and P. Bonderson, Translational symmetry and microscopic constraints on symmetry-enriched topological phases: A view from the surface, *Phys. Rev. X* **6**, 041068 (2016).
- [41] H. G. Evertz, The loop algorithm, *Advances in Physics* **52**, 1 (2003), <https://doi.org/10.1080/0001873021000049195>.
- [42] I. Affleck, D. Gepner, H. Schulz, and T. Ziman, Critical behaviour of spin- s heisenberg antiferromagnetic chains: analytic and numerical results, *Journal of Physics A: Mathematical and General* **22**, 511 (1989).
- [43] R. R. P. Singh, M. E. Fisher, and R. Shankar, Spin-1/2 antiferromagnetic xxz chain: New results and insights, *Phys. Rev. B* **39**, 2562 (1989).
- [44] T. Giamarchi and H. J. Schulz, Correlation functions of one-dimensional quantum systems, *Phys. Rev. B* **39**, 4620 (1989).
- [45] M. Barber, *Phase Transitions and Critical Phenomena*, edited by C. Domb and J. L. Lebowitz, Vol. 8 (Academic Press, London, 1983).
- [46] T. C. Lubensky and M. H. Rubin, Critical phenomena in semi-infinite systems. i. ϵ expansion for positive extrapolation length, *Phys. Rev. B* **11**, 4533 (1975).
- [47] M. Campostrini, M. Hasenbusch, A. Pelissetto, P. Rossi, and E. Vicari, Critical exponents and equation of state of the three-dimensional heisenberg universality class, *Phys. Rev. B* **65**, 144520 (2002).
- [48] Y. Deng, H. W. J. Blöte, and M. P. Nightingale, Surface and bulk transitions in three-dimensional $O(n)$ models, *Phys. Rev. E* **72**, 016128 (2005).
- [49] H. Diehl and S. Dietrich, Scaling laws and surface exponents from renormalization group equations, *Physics Letters A* **80**, 408 (1980).
- [50] H. W. Diehl and A. Nüsser, Critical behavior of the nonlinear σ model with a free surface: The “ordinary” transition in $2+\epsilon$ dimensions, *Phys. Rev. Lett.* **56**, 2834 (1986).
- [51] H. W. Diehl and M. Shpot, Surface critical behavior in fixed dimensions $d < 4$: Nonanalyticity of critical surface enhancement and massive field theory approach, *Phys. Rev. Lett.* **73**, 3431 (1994).
- [52] H. W. Diehl and M. Shpot, Massive field-theory approach to surface critical behavior in three-dimensional systems, *Nuclear Physics B* **528**, 595 (1998).
- [53] F. Gliozzi, P. Liendo, M. Meineri, and A. Rago, Boundary and interface cfts from the conformal bootstrap, *Journal of High Energy Physics* **2015**, 36 (2015).
- [54] H. W. Diehl and S. Dietrich, Field-theoretical approach to multicritical behavior near free surfaces, *Phys. Rev. B* **24**, 2878 (1981).